

Research Article

Dextran-Polyacrylamide as Matrices for Creation of Anticancer Nanocomposite

G. Telegeev,¹ N. Kutsevol,² V. Chumachenko,² A. Naumenko,² P. Telegeeva,¹ S. Filipchenko,² and Yu. Harahuts²

¹*Institute of Molecular Biology and Genetics, National Academy of Sciences of Ukraine, 150 Zabolotnogo Street, Kyiv 03680, Ukraine*

²*Taras Shevchenko National University of Kyiv, 64/13 Volodymyrska Street, Kyiv 01033, Ukraine*

Correspondence should be addressed to N. Kutsevol; kutsevol@ukr.net

Received 28 February 2017; Accepted 18 April 2017; Published 18 May 2017

Academic Editor: Xin Ji

Copyright © 2017 G. Telegeev et al. This is an open access article distributed under the Creative Commons Attribution License, which permits unrestricted use, distribution, and reproduction in any medium, provided the original work is properly cited.

Drug targeting to specific organs and tissues is one of the crucial endeavors of modern pharmacotherapy. Controlled targeting at the site of action and reduced time of exposure of nontargeted tissues increase the efficacy of the treatment and reduce toxicity and side effects, improving compliance and convenience. Nanocarriers based on the branched copolymers dextran-graft-polyacrylamide were synthesized and characterized and were tested on phagocytic cells. It was shown that these nanoparticles are actively captured by phagocytic cells and that they are not cytotoxic. The polymer nanoparticles loaded with cisplatin at different concentrations from 0.1 to 10 $\mu\text{g}/\text{mL}$ yielded dose-dependent decrease in viability of chronic myelogenous leukemia and histiocytic lymphoma cells. The lowest percentage of viable cells was observed for lymphoma cells (22%). Taking into account the fact that our nanoparticles will act mainly on malignant phagocytic cells and do not affect healthy cells, they can thus potentially be used for the therapeutic treatment of tumor cells having phagocytic activity. The effect of nanosilver on cell viability was lower than the one of polymer/cisplatin composite. The data from the cytotoxic studies indicate that nanosilver induces toxicity in cells. However, when the copolymers were conjugated to both nanosilver and cisplatin, such a nanosystem displayed less cytotoxic effect compared to the conjugates of dextran-polyacrylamide and cisplatin.

1. Introduction

Currently, cancer research is focused on improving cancer diagnostic and treatment methods and nanotechnology, which involves the design characterization, production, and application of nanoscale drug delivery systems [1–5]. Polymeric nanoparticles, nanostructured lipid carries, gold nanoparticles, and cyclodextrin complexes are promising tools for modern anticancer therapy [3, 4]. Recently there has been a considerable interest in the development of approaches for the delivery of drugs directly into the cells of the affected organs, without affecting intact cells [3, 4]. Controlled targeted delivery of the drug reduces the influence on nontarget cells and increases the effectiveness of treatment, reducing the side effects.

Macromolecules of soluble polymers, due to their biocompatibility with living cells and tissues and their possible

load dosage forms, are used as nanocontainers or nanotechnology-based drug delivery systems [4]. The drug can be dissolved, entrapped, encapsulated, or attached to a nanoscale polymer matrix which can be as a nanocontainer for drug delivery systems for clinical application, particularly in oncology [4, 6, 7]. Polymer can improve the stability of drugs and control targeting their delivery, allowing for a constant concentration at the site of a lesion and facilitation drug extravasation into the tumor system, thus reducing side effects [7–10].

Metallic nanoparticles have been recognized to have unique physical and chemical properties based on their quantum size, which lead to a range of interesting biomedical applications, especially as promising agents for cancer therapy [11–13]. Silver nanoparticles (AgNPs) play an important role in nanoscience and nanotechnology, particularly in nanomedicine because of their extraordinary properties,

including chemical stability, conductivity, catalytic activity, antibacterial, antifungal, antiviral, and anti-inflammatory activities. Because of their cytotoxic potential, AgNPs have been extensively investigated in cancer research [14]. However, metallic nanoparticles have a tendency to aggregate due to their large surface energy. Various types of stabilizing agents have been used to prevent nanoparticles from aggregating [15–18]; polymers are among them.

Linear polymers or block-copolymers with hydrophilic and hydrophobic blocks are currently studied as promising approach for therapeutically nanosystems preparation [4, 7–9]. However, the theoretical [19, 20] and experimental studies of branched polymers [21, 22] provide us with a reason to assume that these macromolecules may be the most efficient carriers, because they have a higher local concentration of functional groups capable of reacting with the drug.

Hybrid polymer-inorganic materials have been considered potentially attractive for the purpose of developing of new materials [2] with a broad spectrum of interesting properties. In comparison with organic and inorganic constituents and polymers separately, hybrid materials have a lot of advantages [3–5].

The goal of this study was to create hybrid nanocarriers based on the branched copolymers dextran-polyacrylamide capable of entrapping anticancer therapeutic agents, to test their activity using physiological mechanism of the cell-phagocytosis and to reduce side effect on the intact cells.

2. Materials and Methods

2.1. Polymer Nanocarriers. As a nanocarrier we used a branched copolymer obtained by grafting polyacrylamide (PAA) chains onto dextran ($M_w = 7 \times 10^4$, g mol^{-1}) backbone [23, 24] using a ceric-ion-reduce initiation method. This redox process initiates free radical sites exclusively on the polysaccharide backbone, thus preventing from the formation of homopolymer (PAA).

The details of synthesis, identifications, and analysis of internal polymer structure were described in [23, 24]. The theoretical number of grafting sites per polysaccharide backbone for the sample we used as polymer nanocarrier in the present work was equal to 5, and the related dextran-graft-polyacrylamide copolymer was referred to as D70-g-PAA. The choice of this copolymer among the series of the branched samples synthesized based on our previous research. Namely, this sample was the most efficient polymer matrices for Ag sol in situ synthesis as well as for the nano-scale catalyst preparation [25, 26].

The D70-g-PAA copolymer was saponified by alkaline hydrolysis using NaOH to obtain branched polyelectrolyte, referred to as D70-g-PAA(PE) throughout [27]. The degree of saponification of carbamide groups to carboxylate ones onto PAA-granted chains determined by potentiometric titration was equal to 43% [27].

All polymer samples (the nascent and hydrolyzed ones) were precipitated into an excess of acetone, dissolved in bidistilled water, then freeze-dried, and kept under vacuum for preventing them from additional hydrolysis. Potentiometric titration curves obtained for bidistilled water and for the

nonionic copolymer D70-g-PAA were the same. Thus, it can be concluded that the degree of the hydrolysis of the PAA moiety in the nascent copolymer was virtually zero.

2.2. Nanosystem Ag/Polymer/Cisplatin Preparation. AgNPs were synthesized by reduction of Ag precursor (AgNO_3) dissolved in polymer solution. 2 mL of a 0.1 M AgNO_3 aqueous solution was added to 5 mL of aqueous polymer solution ($C = 1 \times 10^{-3} \text{ g}\cdot\text{cm}^{-3}$) and stirred during 20 min. Then, 2 mL of 0.1 M aqueous solution of NaBH_4 was added. The final aqueous solution was stirred during 30 min. It turned reddish brown; thus the formation of AgNPs was indicated. Then, 1 mL of cisplatin ($C = 0.5 \text{ mg/mL}$) was added dropwise to the 1 mL of initial solution of D-g-PAA-Ag ($C_{\text{polymer}} = 1 \text{ mg/mL}$) under stirring for 30 min. For cytotoxicity experiments basic solution of nanocomposite containing polymer + Ag(0) + cisplatin was diluted by water to achieve appropriate concentration of cisplatin as it was shown in Figures 3 and 4 (x -axis).

2.3. Size-Exclusion Chromatography. SEC analysis was carried out by using a multidetection device consisting of a LC-10 AD Shimadzu pump (throughput 0.5 mL min^{-1} ; Japan), an automatic injector WISP 717+ from Waters (USA), three coupled 30 cm Shodex OH-pak columns (803HQ, 804HQ, and 806HQ; Munich, Germany), a multiangle light scattering detector DAWN F from Wyatt Technology (Germany), and a differential refractometer R410 from Waters. Distilled water containing 0.1 M NaNO_3 was used as eluent. Dilute polymer solutions ($c = 3 \text{ g L}^{-1} < c^* = 1/[\eta]$) were prepared, allowing for neglect of intermolecular correlations in the analysis of light scattering measurements.

2.4. Fourier Transform Infrared (FTIR) Spectroscopy. FTIR spectra were obtained on a Nicolet NEXUS-475 (USA) spectrophotometer in the range $4000\text{--}400 \text{ cm}^{-1}$ using thin films with the thickness $6\text{--}9 \mu\text{m}$. The films were cast from aqueous solutions of polymer with cisplatin and without adding it.

2.5. Transmission Electron Microscopy (TEM). For the sample preparation 400 mesh Cu grids with plain carbon film were rendered hydrophilic by a glow discharge treatment (Elmo, Cordouan Technologies, Bordeaux, France). A $5 \mu\text{L}$ drop was deposited and let to be adsorbed for 1 min and then the excess of solution was removed with a piece of filter paper. The observations of the AgNPs were carried on two TEMs, Tecnai G2 or CM12 (FEI, Eindhoven, Netherlands) and the images were acquired with ssCCD Eagle Camera on the Tecnai and a Megaview SIS Camera on the CM12.

2.6. Cell Culture. J-774 (murine macrophage cell line), K-562 (human chronic myelogenous leukemia cell line), and U-937 (human histiocytic lymphoma cell line) were used in this study. The cell lines were obtained from culture collection of Institute of Molecular Biology and Genetics of National Academy of Science of Ukraine and cisplatin from “EBEVE” (Austria). All cell lines were maintained in DMEM (HyClone) containing 4.00 mM L-glutamine, 4500 mg/mL glucose, and sodium pyruvate. The culture medium was supplemented

with 10% fetal bovine serum (GE Healthcare) and 1% penicillin/streptomycin. The cells were cultured in a humidified atmosphere at 37°C and 5% CO₂. In subculturing J-774 cells Trypsin-EDTA solution (GE Healthcare) was used to detach the cells. K-562 cells were detached by careful pipetting with PBS solution (without Ca²⁺/Mg²⁺).

2.7. Cell Viability Assays. Cell viability was determined using MTT assay. Cells were seeded in 96-well plates at cell density of 1×10^5 cells/mL, 100 μ L/well. The incubation was carried out for 16 hours and the cells were exposed to various concentrations of the nanoparticles (diluted in 100 μ L of complete medium). After 48 h incubation 10 μ L of MTT reagent was added to each well and incubated for 4 h. The optical density was measured at 570 nm using a microplate reader (Bio-TEK instrument, Inc.). The percentage of viable cells was determined by using the following formula:

$$\text{Cell viability} = \left(\frac{\text{OD sample}}{\text{OD control}} \right) \times 100\%. \quad (1)$$

The other method for assessment of toxicity was Trypan Blue assay [28]. Cells were seeded on a 6-well plate and grown for 24 hours until nanoparticles were added at appropriate concentrations. The plate was incubated for 48 hours and after exposure to the nanoparticles the cells (10 μ L of each sample) were mixed with 90 μ L of 0.4% Trypan Blue solution (in PBS). The mixtures stood for 2 minutes before both sides of Goryaev chamber were filled with cell suspension (10 μ L) and viewed under an inverted microscope. The number of viable cells were counted and the percentage of viable cells was calculated (the fraction of the number of viable cells over the total number of cells was multiplied by 100).

2.8. Phagocytic Index and Cells Sorting. The efficiency of absorption of the nanocarrier by a cell culture was determined by evaluating phagocytic index. Phagocytic index (PI) is the percentage of cells that are taken up by phagocytosis out of the total cell number.

The distribution of the phases of the cell cycle and apoptosis level were assessed using a FACSCalibur flow cytometer ("Becton Dickinson," USA) by the method described in [28].

2.9. Statistical Analysis. All data are expressed as mean \pm SD of $n = 3$. Two-sample Student's t -test was used to determine statistical significance of differences between two groups. A significance level was set to 0.05 and $P < 0.05$ was considered statistically significant. Statistical analysis was performed using R 3.1.2 software.

3. Results and Discussions

The branched water soluble copolymer dextran-graft-polyacrylamide in nonionic and anionic form has been used as nanocarriers for targeted delivery of an anticancer drug into tumor cells.

TABLE I: Molecular parameters of polymer-nanocarrier.

Sample	$M_w \times 10^{-6} \text{ g mol}^{-1}$	$R_g, \text{ HM}$	M_w/M_n
D70-g-PAA	2.15	85	1.72

The molecular parameters of the D70-g-PAA copolymer, as determined by size-exclusion chromatography (SEC), are reported in Table I.

SEC indicates that this sample possesses relatively low molecular weight polydispersity and the size of macromolecules is relatively large. It is known that cells-phagocytes can trap the objects of 100–250 nm in size. Thus, the D70-g-PAA copolymer can be used for loading the therapeutic agents capable of killing the damaged cells-phagocytes. The peculiarities of the molecular structure of branched copolymers dextran-graft-polyacrylamide in nonionic and ionic forms are discussed in notes [23, 24]. These copolymers are star-like, consisting of the compact dextran core and long polyacrylamide arms. As was reported [23, 24], the average conformation of grafted PAA chains is controlled by the grafting ratio. For the D70-g-PAA copolymer used in the present research the PAA-grafted chains are highly extended, approaching their tethering point, and recover to a random conformation quite distant from this point.

The branched polyelectrolyte D70-g-PAA(PE) is characterized by an extremely expanded conformation of the grafted chains in solution [27]. Alkaline hydrolysis of D70-g-PAA copolymers was not accompanied by irrelevant processes (the breaking or cross-linking of macromolecules) as was confirmed by SEC analysis of source and saponified samples [27]. The branched polymers, due to their more compact molecular structure, have a higher local concentration of functional groups in comparison to their linear analogs. These structure peculiarities of branched polymers are advantageous for application in nanotechnologies [25, 26].

The D70-g-PAA and D70-g-PAA(PE) copolymers consist of biocompatible components, dextran and polyacrylamide, which are nontoxic and water soluble. Macromolecules of polymers are approximately 100 nm in size with ligands capable of coordinating multivalent metal ions [29]. Hence, our idea was to test them as nanocontainers-carriers for targeted delivery of the highly toxic therapeutic anticancer agent cisplatin.

It was shown that the copolymers-nanocontainers were absorbed by macrophages (Figure 1) and were not cytotoxic. The phagocytic index was equal to 84%. This fact permitted the testing of nanocontainers loaded with the cytotoxic chemotherapy drugs cisplatin on the cells.

Complexes of copolymer D70-g-PAA and an anionic derivative with cisplatin were synthesized. The FTIR spectra of the D70-g-PAA(PE) and D70-g-PAA(PE)/cisplatin in comparison with cisplatin spectrum are shown in Figure 2. One can see the presence of both IR bands of copolymer and cisplatin at the vicinity of 782, 1290, 2848, and 3271 cm^{-1} of resulting spectrum. By comparing these spectra some spectral changes are visible. FTIR spectra of D70-g-PAA(PE) and D70-g-PAA(PE)/cisplatin samples which have two strong bands 1650–1660 cm^{-1} and 1615 cm^{-1} are due to

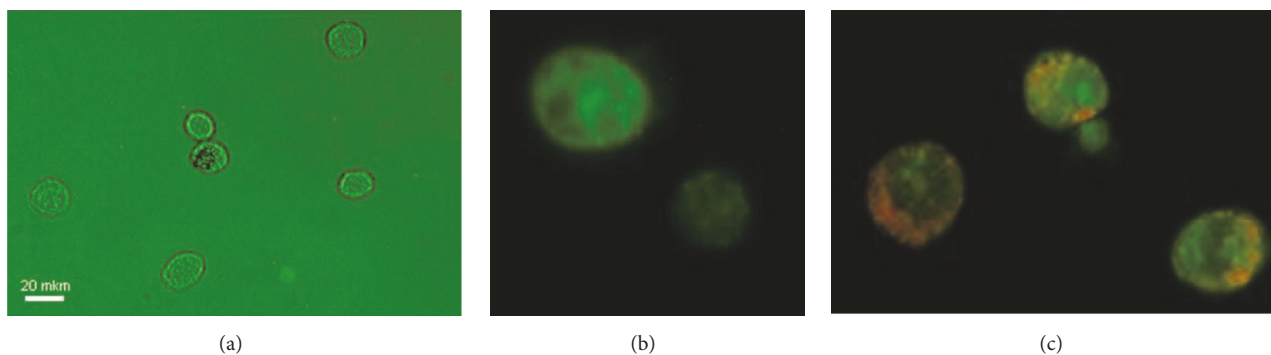


FIGURE 1: Nanocontainers D70-g-PAA tested on murine macrophages. (a) Murine macrophages microphotograph. (b) Murine macrophages under fluorescent microscope without nanocontainers. (c) Murine macrophages with nanocontainers in phagosomes under fluorescent microscope, stained with Acridine Orange.

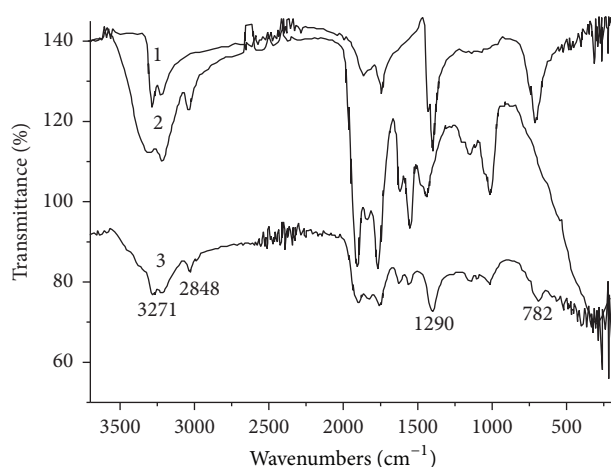


FIGURE 2: FTIR spectra for systems: 1: cisplatin, 2: D70-g-PAA(PE), and 3: D70-g-PAA(PE)/cisplatin.

Amide 1 (C=O stretching) and Amide 2 (N-H bending). The origin of these bands was given in [30]. The spectra of the reaction product of cisplatin with D70-g-PAA(PE) revealed the drastic changes in the intensity of the absorption within Amide I and Amide II bands and for a band with a peak at 1570 cm^{-1} (COO⁻, stretching) [31], respectively, indicating the complex formation of cisplatin with the copolymer carboxyl groups. According to the FTIR data, the system D70-g-PAA(PE)/cisplatin was used in the experiments *in vitro*, giving us the possibility of evaluating our approach.

The cytotoxicity was tested by using both MTT assay and Trypan Blue staining [32]. Dose-dependent cytotoxicity of platinum complexes for J774 cells is shown in Figure 3.

The nanoparticles (D-g-PAA(PE) and those combined with cisplatin) were tested for cytotoxicity by using both MTT assay and Trypan Blue staining [32]. MTT assay was carried out in triplicate and in the range of nanoparticle concentrations from 0.1 to $10\text{ }\mu\text{g/mL}$. Trypan Blue assay also has been done in triplicate but the concentration of $5\text{ }\mu\text{g/mL}$ was used when U-937 and K-562 cells were evaluated for cell viability. The nanoparticles loaded with cisplatin at different

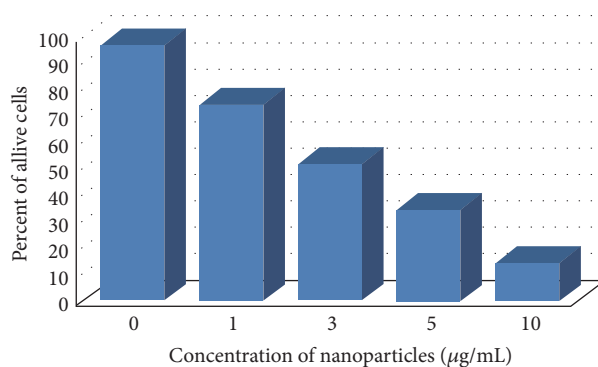


FIGURE 3: Cytotoxicity of nanocontainers combined with cisplatin (D-g-PAA(PE)/cisplatin) for the J774 cells. The data presented here are obtained by using Trypan Blue assay.

concentrations in the range from 1 to $10\text{ }\mu\text{g/mL}$ revealed a percentage of living cells between 28% and 76% for J-774 cell line using Trypan Blue assay.

Staining U-937 and K-562 cells with Trypan Blue after treatment showed that copolymer nanoparticles combined with cisplatin caused decrease in cell viability to about 22% and 39% for U-937 and K-562 cell lines, respectively (Figure 5). MTT test, however, indicated less cytotoxicity for the D-g-PAA(PE)/cisplatin nanoparticles when added to the cells at $10\text{ }\mu\text{g/mL}$ ($\sim 42\%$ for U-937 and $\sim 83\%$ for K-562, Figure 4). Lower ability of K-562 cells to phagocytose solid particles could be an explanation for differences in viability percentage between lymphoma (U 937 culture) and leukemia cells (K 562 culture).

The distribution of the phases of the cell cycle and apoptosis level were assessed using a FACS Calibur flow cytometer [32]. It has been shown that the negative effect of subtoxic concentration of cisplatin (3 mol/L) on the growth of histiocytic lymphoma cells U-937 is the same for both the soluble form of the drug and cisplatin encapsulated into polymer nanoparticles. Thus, cisplatin containing nanoparticles does not lose its growth-inhibitory effect on these cells.

The impact of cisplatin on the cell cycle was also identical when the soluble form of the drug and the drug in

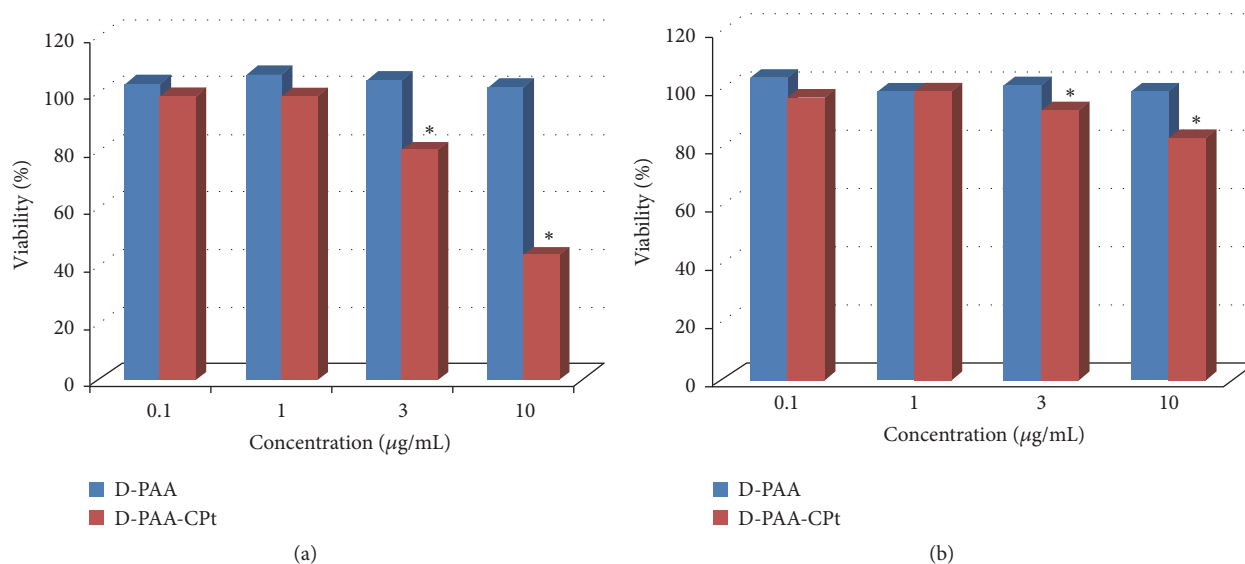


FIGURE 4: Viability (%) of U-937 (a) and K-562 (b) cells after treatment with the nanoparticles (D-g-PAA(PE) and D-g-PAA(PE)/cisplatin) assessed by MTT test. Data are means \pm SD; *significant difference between two groups ($P < 0.05$).

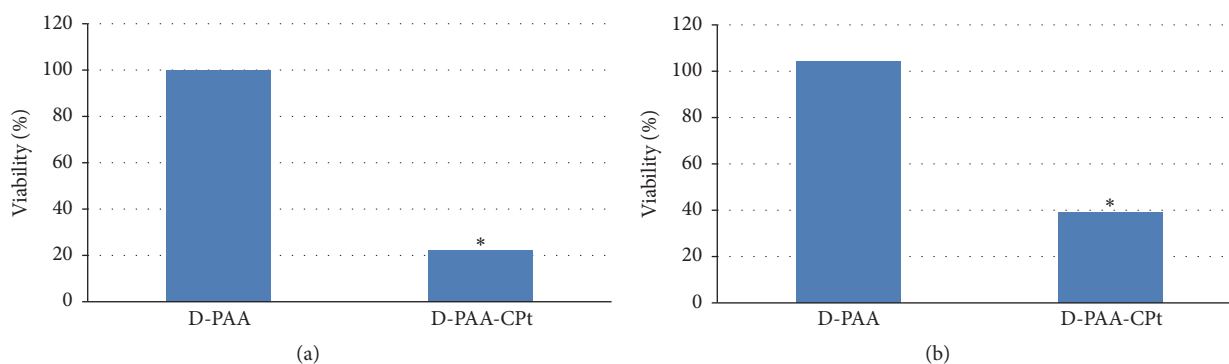


FIGURE 5: The percentage of viable U-937 (a) and K-562 (b) cells after incubation with the nanoparticles D-g-PAA(PE) and D-g-PAA(PE)/cisplatin assessed by Trypan Blue staining. The nanoparticles were added at concentration of 5 μ g/mL D-g-PAA(PE)/cisplatin. Data are means \pm SD; *significant difference between two groups ($P < 0.05$).

nanoparticulate form were added to the cells (increasing fraction of cells in phases S and G2/M). However the level of induction of apoptosis in the preparation form of nanoparticles was somewhat inferior to that under the action of an equimolar concentration of cisplatin solution (Figure 6).

Combining these data with the kinetics of growth culture under treatment with different platinum drugs [33], it could be argued that the effect of cisplatin in the form of nanoparticles on leukemia cells leads to a change in the ratio between the growth-inhibitory and proapoptotic efficacy of platinum at an equimolar content of the active component. In addition, we must take into account the fact that our nanoparticles will act mainly on phagocytic cells and will not affect healthy cells, thus realizing a targeted orientation of nanoparticles with cisplatin.

The next stage of our study was preparation of nanocarrier, containing silver nanoparticles (Polymer/AgNPs) and nanocomposite Polymer/AgNPs/cisplatin.

The first, the binary nanosystem Polymer/AgNPs was synthesized in anionic branched polymer matrix. It should be noted that it was impossible to synthesize stable sol in anionic linear PAA. The branched anionic matrix is a sufficiently rigid structure [27] with extremely extended grafted chains. During silver ion dispersion in a branched polymer matrix followed by their reduction, the charge is partially "neutralized," but the conformation of the branched polymer matrix does not change because, even in the uncharged state, the grafted PAA chains have nearly a worm-like conformation [23]. Due to a partial neutralization of the polymer chain charge during the interaction with silver ions the linear matrix can drastically change its conformation, which, in its turn, increases the possibility of collisions for silver NPs tending to aggregation and some precipitation of AgNPs; however rigid branched molecular structure provides silver particle stabilization.

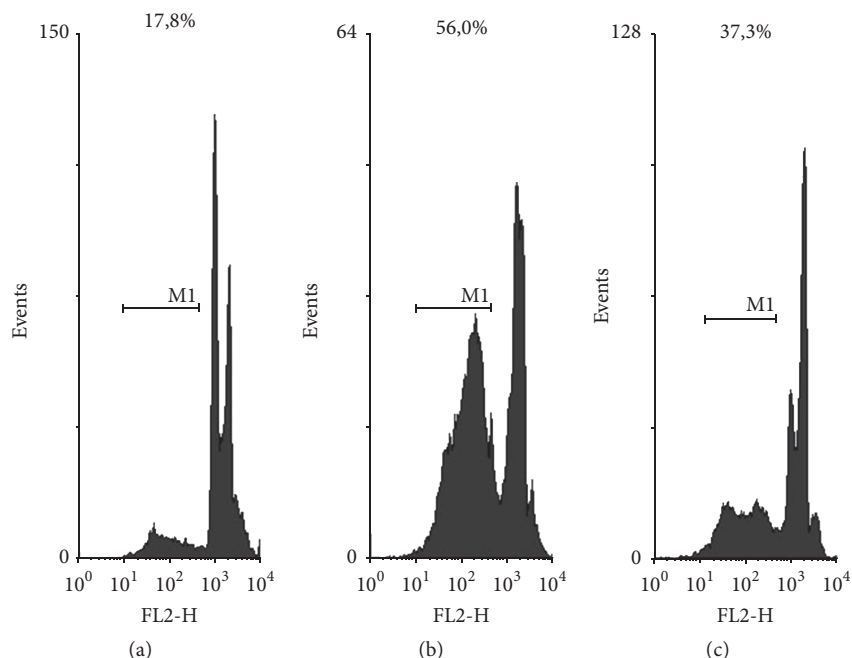


FIGURE 6: Histograms of distribution of U937 cells in content of DNA with the influence of cisplatin in solution or in conjunction with dextran containing nanoparticles: (a) control; (b) cisplatin solution of $3 \mu\text{mol/L}$; (c) nanocontainers loaded with cytotoxic chemotherapy drugs cisplatin, $3 \mu\text{mol/L}$.

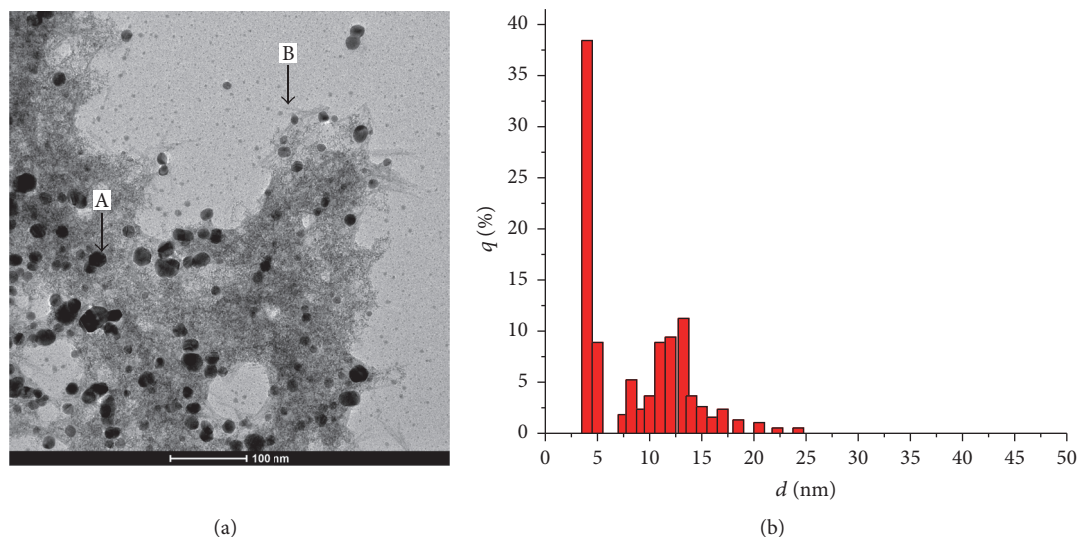


FIGURE 7: TEM image of nanosystem Polymer/AgNPs (a) and histograms of the NP size distribution (b) in the sols synthesized in D-g-PAA(PE) polymer matrix in 2 days after synthesis.

The TEM image of silver sols synthesized in branched anionic polymer matrices and also a histogram of the NP size distribution in this sol are represented in Figures 7(a) and 7(b). Along with NPs (A) with a size of 10–15 nm, NPs with a size of 2–5 nm (B) also formed (Figure 7).

The interaction of silver ions with the anionic polymer matrix takes place with both carbamide (as in nonionic polymers) and carboxylate groups. Moreover, the interaction has the following different mechanisms: the ion-dipole

interaction in the first case and the electrostatic one in the second case. It is supposed that on the carbamide groups of ionic matrices the same particles form as in the nonionic matrices; however the particles on the carboxylated groups are smaller (Figure 7(a) (A; B)) [34].

The TEM image of ternary nanosystem Polymer/AgNPs/cisplatin is shown in Figure 8. It is evident that the AgNPs are the same in size as in binary system Polymer/AgNPs, but some “visualization” of polymer molecules is observed.

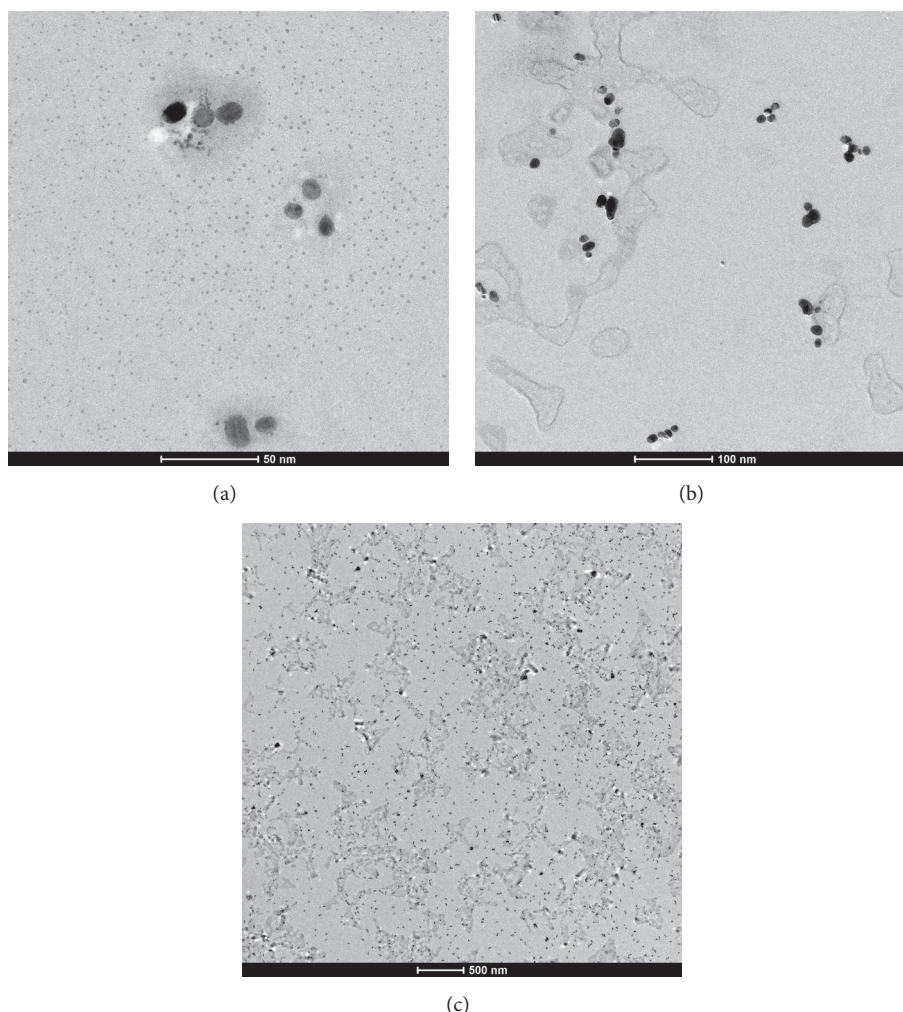


FIGURE 8: TEM image of nanosystem Polymer/AgNPs/cisplatin.

Obviously, cisplatin formed complex with functional groups of polymers matrix and that leads to the partial decreasing of polymer solubility.

The binary and ternary nanosystems were tested on cytotoxic effects (Figures 9(a) and 9(b)). In comparing the results from the assays we notice that a magnitude of an effect for each nanosystem is different. Nevertheless, Trypan Blue data demonstrated a similar tendency of the nanoparticles to induce the cytotoxicity as compared with MTT data. The results of MTT assays also revealed a dose-dependent decrease in viability for both cell lines exposed to either silver or cisplatin conjugated nanoparticles. In the study, as anticipated, copolymers did not exhibit any toxicity to both cell types. At the same time the polymer nanoparticles loaded with cisplatin caused the cytotoxic effect in cell lines at $10 \mu\text{g/mL}$ (40–44% in U-937), and so did silver nanoparticles (Polymer/Ag) at the same concentration (72–76% in U-937 and 86–92% in K-562 provided by MTT assay), although the toxic effect of nanosilver on a cell viability was greater than ones of polymer/cisplatin. The data from the cytotoxic studies indicate that nanosilver induces toxicity in cells. However,

when the copolymers were conjugated to both nanosilver and cisplatin, such a nanosystem displayed less cytotoxic effect compared to the conjugates of dextran-polyacrylamide and cisplatin.

4. Conclusions

The goal of cancer treatment is to kill as many cancer cells as possible without affecting healthy cells. The present research revealed the efficiency of nanodelivery anticancer systems based on the branched copolymer dextran-graft-polyacrylamide and cisplatin. These systems have shown several promising characteristics which can improve traditional chemotherapy. The main advantage of our approach is in target delivery of toxic drugs. It is assumed that it will be used for the treatment of tumor cells possessing phagocytic activity such as leukemia M3–leukemia M5 (acute monocytic leukemia, acute promyelocytic leukemia, acute myelomonocytic leukemia, and FAB classification) without damaging healthy tissue. Our experiment proved that nanocontainers of the particles are nontoxic, which is important in the

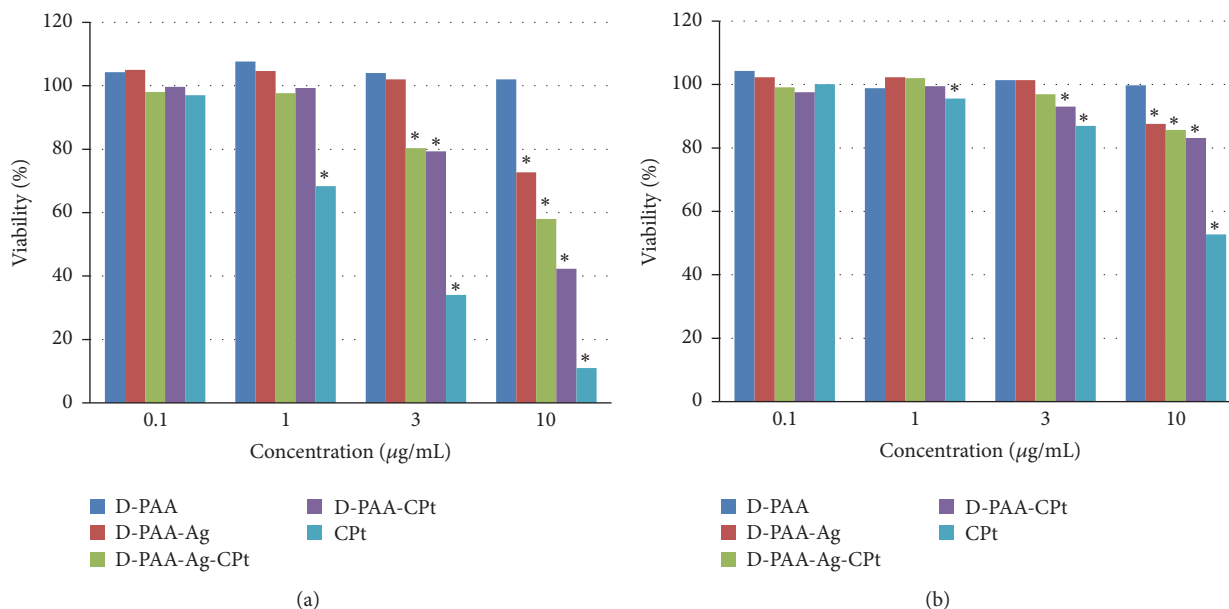


FIGURE 9: Viability of the U-937 cells (a) and K-562 cells (b) after cultivation with the nanoparticles at different concentrations for 48 h measured by MTT assay (a) and Trypan Blue assay (b). Mean values of triplicates with standard deviation are shown. * $P < 0.05$ compared to the untreated control.

therapy session. Further studies are needed to turn concept of nanotechnology into practical application (in vitro and in vivo) and to elucidate correct drug doses and optimal copolymer internal structure for ideal release of therapeutical agent encapsulated in polymer molecule for the treatment of cancer cells.

The effect of nanosilver on cell viability was lower than the one of polymer/cisplatin. The data from the cytotoxic studies indicate that nanosilver induces toxicity in cells. However, when the copolymers were conjugated to both nanosilver and cisplatin, such a nanosystem displayed less cytotoxic effect compared to the conjugates of dextran-polyacrylamide and cisplatin.

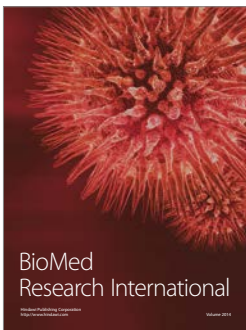
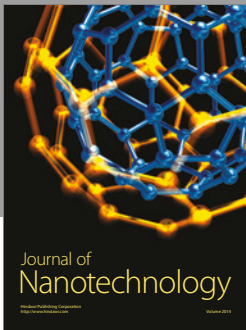
Conflicts of Interest

The authors declare that there are no conflicts of interest regarding the publication of this paper.

References

- [1] S. T. Selvan and K. Narayanan, *Introduction to Nanotheranostics, SpringerBriefs in Applied Sciences and Technology*, Springer, Singapore, 2016.
- [2] N. Martinho, C. Damge, and C. P. Reis, "Recent advances in drug delivery systems," *Journal of Biomaterials and Nanobiotechnology*, vol. 2, no. 5, pp. 510–526, 2011.
- [3] V. J. Mohanraj and Y. Chen, "Nanoparticles—a review," *Tropical Journal of Pharmaceutical Research*, vol. 5, no. 1, pp. 561–573, 2006.
- [4] G. Calixto, J. Bernegossi, B. Fonseca-Santos, and M. Chorilli, "Nanotechnology-based drug delivery systems for treatment of oral cancer: a review," *International Journal of Nanomedicine*, vol. 9, no. 1, pp. 3719–3735, 2014.
- [5] J. R. Lattin, D. M. Belnap, and W. G. Pitt, "Formation of eLiposomes as a drug delivery vehicle," *Colloids and Surfaces B: Biointerfaces*, vol. 89, no. 1, pp. 93–100, 2012.
- [6] Y. Liu, H. Miyoshi, and M. Nakamura, "Nanomedicine for drug delivery and imaging: a promising avenue for cancer therapy and diagnosis using targeted functional nanoparticles," *International Journal of Cancer*, vol. 120, no. 12, pp. 2527–2537, 2007.
- [7] L. E. van Vlerken and M. M. Amiji, "Multi-functional polymeric nanoparticles for tumour-targeted drug delivery," *Expert Opinion on Drug Delivery*, vol. 3, no. 2, pp. 205–216, 2006.
- [8] J. K. Vasir and V. Labhasetwar, "Biodegradable nanoparticles for cytosolic delivery of therapeutics," *Advanced Drug Delivery Reviews*, vol. 59, no. 8, pp. 718–728, 2007.
- [9] K. S. Soppimath, T. M. Aminabhavi, A. R. Kulkarni, and W. E. Rudzinski, "Biodegradable polymeric nanoparticles as drug delivery devices," *Journal of Controlled Release*, vol. 70, no. 1-2, pp. 1–20, 2001.
- [10] M. Ferrari, "Cancer nanotechnology: opportunities and challenges," *Nature Reviews Cancer*, vol. 5, no. 3, pp. 161–171, 2005.
- [11] S. Jain, D. Hirst, and J. O'Sullivan, "Gold nanoparticles as novel agents for cancer therapy," *British Journal of Radiology*, vol. 85, no. 1010, pp. 101–113, 2012.
- [12] R. Arvizo, R. Bhattacharya, and P. Mukherjee, "Gold nanoparticles: opportunities and challenges in nanomedicine," *Expert Opinion on Drug Delivery*, vol. 7, no. 6, pp. 753–763, 2010.
- [13] C. Yao, L. Zhang, J. Wang et al., "Gold nanoparticle mediated phototherapy for cancer," *Journal of Nanomaterials*, vol. 2016, Article ID 5497136, 29 pages, 2016.
- [14] X. Zhang, Z. Liu, W. Shen, and S. Gurunathan, "Silver nanoparticles: synthesis, characterization, properties, applications, and therapeutic approaches," *International Journal of Molecular Sciences*, vol. 17, no. 9, p. 1534, 2016.

- [15] D. Huang, G. Yang, X. Feng, X. Lai, and P. Zhao, "Triazole-stabilized gold and related noble metal nanoparticles for 4-nitrophenol reduction," *New Journal of Chemistry*, vol. 39, no. 6, pp. 4685–4694, 2015.
- [16] J. Hu, Q. Yang, L. Yang et al., "Confining noble metal (Pd, Au, Pt) nanoparticles in surfactant ionic liquids: active non-mercury catalysts for hydrochlorination of acetylene," *ACS Catalysis*, vol. 5, no. 11, pp. 6724–6731, 2015.
- [17] Z. Wang, B. Tan, I. Hussain et al., "Design of polymeric stabilizers for size-controlled synthesis of monodisperse gold nanoparticles in water," *Langmuir*, vol. 23, no. 2, pp. 885–895, 2007.
- [18] V. Thomas, M. Namdeo, Y. M. Mohan, S. K. Bajpai, and M. Bajpai, "Review on polymer, hydrogel and microgel metal nanocomposites: a facile nanotechnological approach," *Journal of Macromolecular Science, Part A: Pure and Applied Chemistry*, vol. 45, no. 1, pp. 107–119, 2008.
- [19] G. S. Grest, L. J. Fetters, J. S. Huang, and D. Richter, "Star polymers: experiment, theory, and simulation," *Advances in Chemical Physics*, vol. 94, pp. 67–163, 1996.
- [20] M. Ballauff, "Spherical polyelectrolyte brushes," *Progress in Polymer Science (Oxford)*, vol. 32, no. 10, pp. 1135–1151, 2007.
- [21] G. Widawski, M. Rawiso, and B. François, "Self-organized honeycomb morphology of star-polymer polystyrene films," *Nature*, vol. 369, no. 6479, pp. 387–389, 1994.
- [22] M. Heinrich, M. Rawiso, J. G. Zilliox, P. Lesieur, and J. P. Simon, "Small-angle X-ray scattering from salt-free solutions of star-branched polyelectrolytes," *European Physical Journal E*, vol. 4, no. 2, pp. 131–142, 2001.
- [23] N. Kutsevol, J.-M. Guenet, N. Melnik, D. Sarazin, and C. Rochas, "Solution properties of dextran-polyacrylamide graft copolymers," *Polymer*, vol. 47, no. 6, pp. 2061–2068, 2006.
- [24] N. Kutsevol, T. Bezugla, M. Bezuglyi, and M. Rawiso, "Branched dextran-graft-polyacrylamide copolymers as perspective materials for nanotechnology," *Macromolecular Symposia*, vol. 317–318, no. 1, pp. 82–90, 2012.
- [25] M. Bezuglyi, N. Kutsevol, M. Rawiso, and T. Bezugla, "Water-soluble branched copolymers dextran-polyacrylamide and their anionic derivatives as matrices for metal nanoparticles in situ synthesis," *Chemik*, vol. 66, no. 8, pp. 865–867, 2012.
- [26] V. Chumachenko, N. Kutsevol, M. Rawiso, and C. Schmutz, "In situ formation of silver nanoparticles in linear and branched polyelectrolyte matrices using various reducing agents," *Nano-scale Research Letters*, vol. 9, article 164, 2014.
- [27] N. Kutsevol, M. Bezuglyi, T. Bezugla, and M. Rawiso, "Star-like dextran-graft-(polyacrylamide-co-polyacrylic acid) copolymers," *Macromolecular Symposia*, vol. 335, no. 1, pp. 12–16, 2014.
- [28] I. Nicoletti, G. Migliorati, M. C. Pagliacci, F. Grignani, and C. Riccardi, "A rapid and simple method for measuring thymocyte apoptosis by propidium iodide staining and flow cytometry," *Journal of Immunological Methods*, vol. 139, no. 2, pp. 271–279, 1991.
- [29] N. Kutsevol, A. Naumenko, and V. Chumachenko, "Comparison of branched and linear anionic Polyacrylamide flocculants on removal of heavy metal ions from Kaolin dispersion," in *Proceedings of the 38th AMOP Technical Seminar on Environmental Contamination and Response*, pp. 340–350, Canada, June 2015.
- [30] B. R. Nayak and R. P. Singh, "Synthesis and characterization of grafted hydroxypropyl guar gum by ceric ion induced initiation," *European Polymer Journal*, vol. 37, no. 8, pp. 1655–1666, 2001.
- [31] S. Kiatkamjornwong, W. Chomsaksakul, and M. Sonsuk, "Radiation modification of water absorption of cassava starch by acrylic acid/acrylamide," *Radiation Physics and Chemistry*, vol. 59, no. 4, pp. 413–427, 2000.
- [32] W. Strober, "Trypan blue exclusion test of cell viability," *Current Protocols in Immunology*, 2001, Appendix 3:Appendix 3B.
- [33] X. Wang and Z. Guo, "Targeting and delivery of platinum-based anticancer drugs," *Chemical Society Reviews*, vol. 42, no. 1, pp. 202–224, 2013.
- [34] N. V. Kutsevol, V. A. Chumachenko, M. Rawiso, V. F. Shkodich, and O. V. Stoyanov, "Star-like dextran-polyacrylamide polymers: Prospects of use in nanotechnologies," *Journal of Structural Chemistry*, vol. 56, no. 5, pp. 959–966, 2015.



Hindawi

Submit your manuscripts at
<https://www.hindawi.com>

